International Communications in Heat and Mass Transfer 128 (2021) 105604

Contents lists available at ScienceDirect

International Communications in Heat and Mass Transfer

journal homepage: www.elsevier.com/locate/ichmt

Dynamics of viscoelastic fluid conveying nanoparticles over a wedge when bioconvection and melting process are significant

M. Ijaz Khan [a,b,*], Faris Alzahrani [b]

[a] Department of Mathematics and Statistics, Riphah International University I-14, Islamabad 44000, Pakistan
[b] Nonlinear Analysis and Applied Mathematics (NAAM)-Research Group, Department of Mathematics, Faculty of Sciences, King Abdulaziz University, P.O. Box 80203, Jeddah 21589, Saudi Arabia

ARTICLE INFO

Keywords:
Second-grade nanofluid
Activation energy
Falkner–Skan flow
Non-uniform heat source/sink
Bioconvection

ABSTRACT

The research in nanoparticles presents a convincing attention of scienstis due to their interesting applications in nanotechnology, electrical and biomedical, biotechnology, medication delivery, chemotherapy, food processing, and other sectors. The investigation presents the applications of viscoelastic nanoparticles with moving microorganisms due to wedge-shaped geometry. The important features of activation energy, thermophoresis diffusion characteristics and Brownian motion are also highlighted. The analysis is performed in view of Melting process. The flow process is represented mathematically using partial differential equations. For the optimization technique using MATLAB computer-based tools, the Labotto IIIa formulation has utilized. In the velocity equation, the temperature profile, concentration profile and microorganisms' profile, the reporting of the main parameters are fully defined and discussed through figures. The speed can be enhanced by means of a mixed convection appearance is determined. Furthermore, nanoparticles are decreasing in temperature and concentration profiles and the high number of Peclet decreases the profile of microorganisms.

1. Introduction

Following to the remarkable thermodynamic characteristics, substantial research efforts in recent years on nanofluids are being made. Air conditioning, high-flow equipment, laundry washing equipment, high-power microwave stoves, height-powered laser diode range and a number of welding machines are available in the usage of nanofluids. Furthermore, substantial advances in nanotechnology have opened up the possibility of utilizing magnetic nanoparticles to treat brain tumors, pharmaceutical treatments, artificial heart surgery, artificial lungs, cancer therapy, and other conditions. Sophisticated nanotechnology has offered various beneficial approaches aimed at the interaction of nanomaterials in order to increase the usage of fossil fuels and relieve environmental problems. Choi [1] developed the fundamental notion of these nano-materials with enhanced thermophysical properties, which was further extended by other researchers. Nano-materials have a high potential for increasing heat transformation characteristics. Nonliquid has the greatest thermal conductivity associated with the base liquid. The material is used in industrial and engineering fields such as electronic cooling machines, nano suits, and other industries. In actuality, nanofluids are used in nano-materials made of metals, oxides, jets, heat transformation mechanisms, nuclear reactors, and refrigeration electrical devices, as well as heating systems, medicines, nano-tubes, and carbon steels. The crucial significance of non-homogeneous experimental consistency for natural circulation modification of convectional nano-materials was studied by Buongiorno et al. [2]. He developed adequate procedures for sliding Brownian diffusion and thermophoresis. Lahmar et al. [3] examined the reality that thermal conductivity depends on the temperature and the presence of the inclination magnetization field for compressed, unstable nanofluids between two parallel plates. Fatunmbi et al. [4] investigated the temperature and concentration distribution characteristics of Nonlinear Thermal Radiation using an Eying-Powell nanofluid through a vertical porous plate and exponentially rising viscosity in the porous material. Shafiq et al. [5] investigated the Magnetohydrodynamic mobility and heat transmission of nanotubes reliant on carbon-based nanofluid over a variable thickness sheet. Loganathan et al. [6] investigated the MHD thermal radiation Williamson flow of nanofluid produced by an expanding surface encased in a porous channel via Joule heating, natural convection heating, and mechanical nanoparticle function. Physical observations on the Two-Dimensional Mixed magnetic convective flowing Nonliquid Casson on a vertically spinning small needle without nonlinear Thermal Radiation

* Corresponding author at: Department of Mathematics and Statistics, Riphah International University I-14, Islamabad 44000, Pakistan.
E-mail address: mikhan@math.qau.edu.pk (M.I. Khan).

https://doi.org/10.1016/j.icheatmasstransfer.2021.105604

Available online 17 September 2021

and Heat Source/Senk effects were conducted by Hamid et al. [7]. Aman et al. [8] simulated fractional derivative procedure to present the nanofluid problem solution. Turkyilmazoglu [9] successfully pointed out the stability criteria in single phase nanofluid model flow. Ellahi et al. [10] focused on the thermal aspects of slip flow of nanofluid problem by using the hafnium particles. Abbas et al. [11] investigated the thermally developed nanoparticles prospective over stretched cylinder. Nadeem et al. [12] presented dual numerical solution for nanofluid flow following the stagnation point applications. Shehzad et al. [13] imposed the magnetic impact while inspecting the thermal change in viscoelastic nanofluid problem. Ikram et al. [14] discussed the heat transfer improvement by using the hybrid nanoparticles in parallel plates flow. The optimized performances of Williamson nanofluid with dissipation significances was directed in the analysis of Qayyum et al. [15]. Hosseinzadeh et al. [16] analyzed the bio-convective phenomenon in the cross nanofluid flow with three-dimensional stretched surface. Khan [17] worked on the forced convective transport of nanofluid due to rotating disk. Song et al. [18] predicted the thermal change in the ethylene glycol base fluid with immersion of nanoparticles due to heated surface. Oke et al. [19] observed the aspects of Coriolis forces for nanoparticles flow in a uniform sphere. Li et al. [20] addressed the second order slip consequences for the nanofluid flow numerically. Animasaun et al. [21] surmised the dynamic of tinay nanoparticles following the haphazard motion. Wakif et al. [22] performed the meta-investigation regarding the nanoparticles motion with viscous base fluid. Shah et al. [23] tested the temperature gradient impact on the nanofluid flow numerically. Sowmya et al. [24] addressed the thermal out comes for the silver and iron oxide nanoparticles with buoyancy force applications. Makinde and Animasaun [25] visualized the aspects of quartic autocatalysis for nanofluid thermal flow in paraboloid of revolution. In another analysis Makinde and Animasaun [26] discussed the bio-convective transport of nanofluid subject to the quartic chemical features.

The phenomenon of bioconvection occurs when a motile microbe that is as large as a microorganism in the water swims upward. As a significant biofuel process, bioconvection has emerged. Bioconvection for biofuel, fertilizer and industrial processes has been applied. The research on density stratification, pattern formation owing to microbiomes, nano-material and booster internships was conducted at nanofluid bioconvection. Low algae and other oxytactic bacteria, two types of upwelling microorganisms, are commonly used in bioconvection science. Although the structure of bioconvection is quite similar, the orientation systems vary. Swimming in calm water is preferred owing to the asymmetrical distribution of low-mass bacteria. When these microorganisms are in motion, the direction of swimming is determined by the balance of toques generated by viscous dissipation drag caused by shear motion and gravity pressing on the cell. Kuznetsov [27] investigated the evolution of nanofluid bioconvection in suspensions, including microorganisms and nanotechnology. Nayak et al. [28] investigated the effects of momentum, temperature, solutal, and microorganism sliding on the flow of biologically inert nanofluid using an electromagnetic stretching surface. Chemical reaction occurrences have layers. Khan et al. [29] investigated bioconvection's influence on the rheology of the magnetization pair of nanofluid tension with energy activation. Magagula et al. [30] examined the understanding of the Casson's nano fluid stream across the extended surface, which is a two-dispensed gyrotactic microbe. Beg et al. [31] studied the non-linearity-inclined expanded area under non-uniform magnetic fields for computing conductive bioconvection. In comparison with the deferment point of small particles above delayed sheets, Mamatha et al. [32] assessed the mass transformation of the constant incompressible magnetic-hydrodynamic bioconvective fluid flow. Nima et al. [33] examined the effects of melting in non-Newtonian fluid flowing through non-Darcy porous materials having varied fluid flow characteristics in bio-convective swimming microorganisms. Ramzan et al. [34] investigated the importance of hall impacts and ion slides on stretch surfaces in the 3D bioconvection hyperbolic nano lytic flow under Arrhenius energy of activation. Tlili et al. [35] examined the effect on second-order bioconvection of slip-on nanofluid. Some more recent analysis regarding the various models with and without nanofluid can be seen in refs. [36–40].

The melting flow of viscoelastic nanofluid has been studied in presence of microorganisms. The induced flow is caused by a moving wedge. The activation energy consequences are also elaborated. This research communicates the answer of following research questions [23,24]:

- What is the impact of melting heat transfer phenomenon in the wedge flow of viscoelastic nanofluid?
- How the stability of nanoparticles is improved with the enrolment of microorganism?
- How the concentration of viscoelastic nanoparticles improved with the activation energy phenomenon?

The importance of activation energy is also taken into consideration. The MATLAB computational software bvp4c can solve the dimensionless ODE modeled nanofluid of second grade numerically (Labotto IIIa formula). Visual and quantitative behavior is important considerations.

2. Mathematical description of flow problem

Let us examine a 2-D Falkner Skan flow of second grade fluid with swimming microorganisms over a moving wedge. The wedge velocity is denoted with $U_w(x) = bx^n$ with stretching rate b. At free stream space, the velocity of wedge is expressed with $U_e(x) = ex^n$. The nanofluid temperature, concentration and motile density are symbolized with T, C and N, respectively. The activation energy relations are encountered in the concentration equation. The melting applications are also introduced. The governing equations for modeled problem are:

$$u_x + v_y = 0, \tag{1}$$

$$\begin{aligned} uu_x + vu_y = {} & vu_{yy} + \frac{\alpha_1^*}{\rho}\left[u_x u_{yy} + u_{yyx} - u_y v_{yy} + vu_{yyy}\right] \\ & + U_e\frac{dU_e}{dx} - \frac{\sigma B_0^2}{\rho} sin^2\psi(u - U_e) \\ & + \frac{1}{\rho_f}\left[(1 - C_f)\rho_f\beta^* g(T - T_\infty) - (\rho_p - \rho_f)g(C - C_\infty) - (N \right. \\ & \left. - N_\infty)g\gamma^{**}(\rho_m - \rho_f)\right], \end{aligned} \tag{2}$$

$$uT_x + vT_y = \alpha_m T_{yy} + \tau\left[D_B T_y C_y + \frac{D_T}{T_\infty}(T_y)^2\right], \tag{3}$$

$$uC_x + vC_y = D_B C_{yy} + \frac{D_T}{T_\infty}T_{yy} - Kr^2(C - C_\infty)\left(\frac{T}{T_\infty}\right)^n exp\left(\frac{-E_a}{kT}\right), \tag{4}$$

$$uN_x + vN_y = D_m(N_{yy}) - \frac{bW_c}{(C_w - C_\infty)}\left[N_y C_{yy}\right], \tag{5}$$

$$\left.\begin{aligned} & u = U_w(x) = bx^n, \mu\frac{\partial u}{\partial y}\Big|_{y=0}\frac{\partial\sigma}{\partial x}\Big|_{y=0} = \frac{\partial\sigma}{\partial T}\frac{\partial T}{\partial x}\Big|_{y=0} - \frac{\partial\sigma}{\partial C}\frac{\partial C}{\partial x}\Big|_{y=0}, \\ & -k\frac{\partial T}{\partial y} = h_f(T_w - T), D_B C_y + \frac{D_T}{T_\infty}T_y = 0, N = N_m \, at \, y = 0, \\ & u = U_e(x) = ex^n, T\to T_\infty, C\to C_\infty, N\to N_\infty, \text{as y}\to\infty, \end{aligned}\right\} \tag{6}$$

where (u,v) velocity is shown along $(x$ & $y)$ the direction, the temperature is (T) shown, the Brownian diffusion coefficient is (N_B) represented, the material fluid parameter is $(\alpha_1{}^*)$, (C)indicated by the concentration, the fluid latent thermal is (λ) indicated and fluid density is (ρ) indicated, (C_∞) is the concentration of fluid in the atmosphere, the kinematic viscosity is(υ) indicated, electric conductivity is represented (σ), the surface heat capability is indicated. The individual heat (C_p), the

thermal fluid conductivity (k), the heat diffusion coefficient is (D_T), the microorganisms (N), the ambient fluid temperature is (T_∞) and ambient fluid microorganisms are (N_∞), the specific fluid thermal conductivity is (k).

$$\left.\begin{array}{l}\zeta\left(=\frac{(n+1)U_e}{2vx}\right)^{\frac{1}{2}}y,\psi\left(=\frac{2vxU_e}{n+1}\right)f(\zeta),\\ \theta(\zeta)\left(=\frac{T-T_m}{T_\infty-T_m}\right),\phi(\zeta)\left(=\frac{C-C_m}{C_\infty-C_m}\right),\chi(\zeta)\left(=\frac{N-N_m}{N_\infty-N_m}\right),\end{array}\right\} \tag{7}$$

The dimensional form of governing equations is:

$$f''' + \left(\frac{2n}{n+1}\right)\left(1-f'^2\right) + ff'' + \alpha_1\left[(3n-1)f'f''' + \left(\frac{3n-1}{2}\right)f''^2 + (n-1)\zeta f''f''' - \left(\frac{n+1}{2}\right)ff^{iv}\right] - (M)^2 sin^2\psi(f'-1) - \lambda(\theta - Nr\phi - Nc\chi) = 0, \tag{8}$$

$$\theta'' + Prf\theta' + PrNb\theta'\phi' + PrNt\theta'^2 = 0, \tag{9}$$

$$\frac{1}{Sc}\phi'' + f\phi' + \frac{Nt}{Nb}\theta'' - PrLe\sigma^*(1+\delta\theta)^n exp\left(\frac{-E}{(1+\delta\theta)}\right)\phi = 0, \tag{10}$$

$$\chi'' + Lbf\chi' - Pe(\phi''(\chi+\delta_1) + \chi'\phi') = 0, \tag{11}$$

With

$$\left.\begin{array}{l}f(\zeta)=0, f'(\zeta)|_{\zeta=0} = -Q(1+Ma), \theta'(0) = -Bi(1-\theta(0)),\\ \phi(\zeta)=0, Nb\phi'(\zeta) + Nb\theta'(\zeta) = 0 \, at \, \zeta = 0,\\ f'(\zeta)\to 1, \theta(\zeta)\to 1, \phi(\zeta)\to 1, \chi(\zeta)\to 1, as\, \zeta\to\infty\end{array}\right\} \tag{12}$$

Here, involved physical parameters are listed as (E)stand for activation energy parameter, (M)is a magnetic parameter, (Nc) is for bioconvection Rayleigh number,(Lb)depicts the bioconvection Lewis number,(Nr)depicts buoyancy ratio parameter, (Nt)shows thermophoresis parameter, (Pr)stand for Prandtl number, (Nb) display Brownian motion parameter, (Pe)is Peclet number, (λ) is mixed convection parameter, (σ)is chemical reaction parameter, (α) the wedge angle parameter, (δ)signifies the temperature difference parameter, (δ_1) is microorganism difference parameter, (Le)is Lewis number, (τ)stand for thermophoretic parameter,(n) wedge parameter,(β) the second-grade fluid parameter, (Q)Marangoni number, and (Ma) Marangoni ratio parameter.

$$\left.\begin{array}{l}\lambda = \frac{\beta^* g(1-C_\infty)(T_w-T_\infty)}{(m+1)u_e^2}, Nr = \frac{(\rho_p-\rho_f)(C_w-C_\infty)}{(1-C_\infty)(T_w-T_\infty)\beta^*}, Ma\left(=\frac{\gamma_C B}{\gamma_T A}\right),\\ Nc = \frac{\gamma^{**}(\rho_m-\rho_f)(N_w-N_\infty)}{(1-C_\infty)\left(T_w-\widetilde{T}_\infty\right)\beta}, Pr = \frac{v}{\alpha_m}, Nb = \frac{\tau D_B(C_w-C_\infty)}{\nu},\\ Nt = \frac{\tau D_T(T_w-T_\infty)}{T_\infty\nu}, E = \frac{E_a}{kT_\infty}, \sigma = \frac{kr^2}{a}, \delta = \frac{T_w-T_\infty}{T_\infty},\\ Pe = \frac{bW_c}{D_m}, \mathrm{Lb} = \frac{\nu}{D_m}, \delta_1 = \frac{N_\infty}{N_w-N_\infty}, Le = \frac{\alpha}{D_B}, \tau = \frac{K_T(T_w-T_\infty)}{T_r},\\ \alpha = \frac{Q_0 S}{\rho C_p a x^{n-1}}, \beta = \frac{\alpha_1^* a x^{n-1}}{\mu}, M^2 = \frac{\sigma B_0^2}{\rho a x^{n-1}}, Q = \frac{\gamma_T A}{\mu\Omega}\sqrt{\frac{\Omega}{\gamma}}\end{array}\right\} \tag{13}$$

The physical quantities are as follows:

$$C_f = \frac{2\tau_{xy}}{\rho U_w^2}, \tau_{xy} = \mu u_y\big|_{y=0} + \alpha_1^*\left(uu_{yx} + vu_{yy} + 2u_x u_y\right)_{y=0}. \tag{14}$$

$$(Re_x)^{\frac{1}{2}}C_f = f''(0) - \alpha_1(n + 2/2A + n + 1/2f(0))f'(0) \tag{15}$$

$$Nu_x = xq_w/k(T_\infty - T_m), q_w = -kT_y\big|_{y=0}. \tag{16}$$

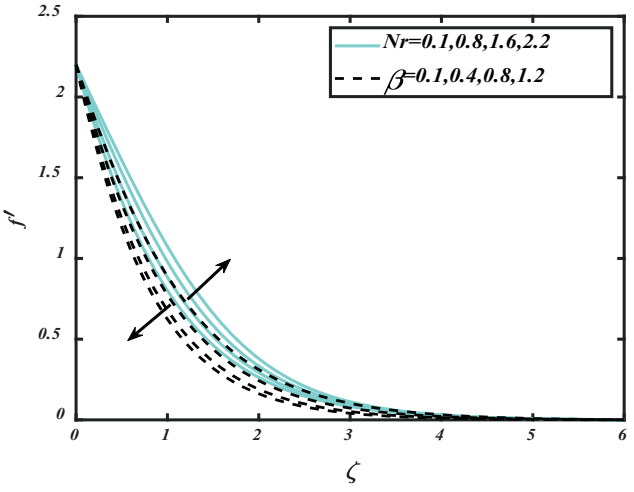

Fig. 1. f'against Nr & β.

$$(Re_x)^{\frac{-1}{2}}Nu_x = -\theta'(0) \tag{17}$$

3. Solution via shooting scheme

The reduced ordinary differential that fixes these problems in many scientific, engineering, biological and industrial settings is very nonlinear, posing problems for scientists, scientists and mathematicians. These flux models are quantitatively discussed. A 3-stage LobattoIIIa screening approach in computer program with MATLAB software. By following a number of additional variables, the higher-ordre BVP is converted to the first-order IVP.

Let

$$\left.\begin{array}{l}f = h_1, f' = h_2, f'' = h_3, f''' = h_4, f^{iv} = h_4'\\ \theta = h_5, \theta' = h_6, \theta'' = h_6',\\ \phi = h_7, \phi' = h_8, \phi'' = h_8',\\ \chi = h_9, \chi' = h_{10}, \chi'' = h_{11}',\end{array}\right\} \tag{18}$$

$$h_4' = h_4 + \left(\frac{2n}{n+1}\right)\left(1-h_2^2\right) + h_1h_3 - (Ha)^2 sin^2\psi(h_2-1) - \lambda(h_5 - Nrh_7 - Nch_9) + \alpha_1\left[(3n-1)h_2h_4 + \left(\frac{3n-1}{2}\right)h_3^2 + (n-1)\zeta h_3h_4\right] \Big/ \alpha_1\left(\tfrac{n+1}{2}\right)h_1, \tag{19}$$

$$h_6' = -Prh_1h_6 - PrNbh_6h_8 - PrNth_6^2, \tag{20}$$

$$h_8' = LePr\left(-h_1h_8 - \frac{Nt}{Nb}h_6', + PrLe\sigma^*(1+\delta h_5)^n exp\left(\frac{-E}{(1+\delta h_5)}\right)h_7\right), \tag{21}$$

$$h_{11}' = -Lbh_1h_{10} + Pe\left(h_8'(h_9+\delta_1) + h_{10}h_8\right), \tag{22}$$

With

$$\left.\begin{array}{l}h_1(\zeta)=0, h_2(\zeta)|_{\zeta=0} = -1Q(1+Ma), h_6(0) = -Bi(1-h_5(0)),\\ h_7(\zeta)=0, Nbh_8(\zeta) + Nbh_6(\zeta) = 0 \, at \, \zeta = 0,\\ h_2(\zeta)\to 1, h_5(\zeta)\to 1, h_7(\zeta)\to 1, h_9(\zeta)\to 1, as\, \zeta\to\infty\end{array}\right\}, \tag{23}$$

4. Graphical findings and discussion

In the following sections, we will explore in detail the impacts of the flux-speed parameters, the second-grade temperature profile of

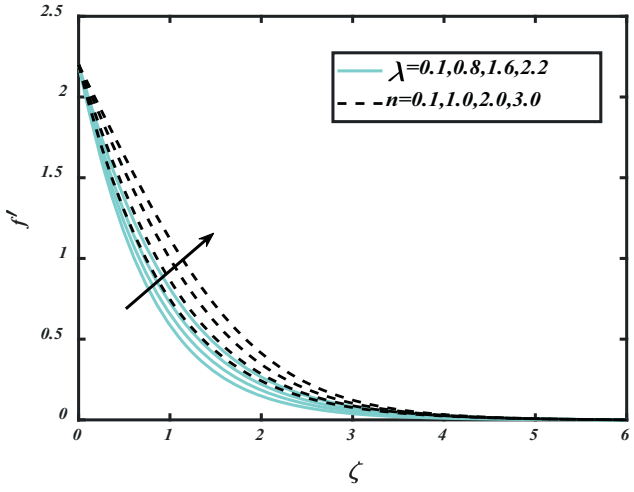

Fig. 2. f' against λ & n.

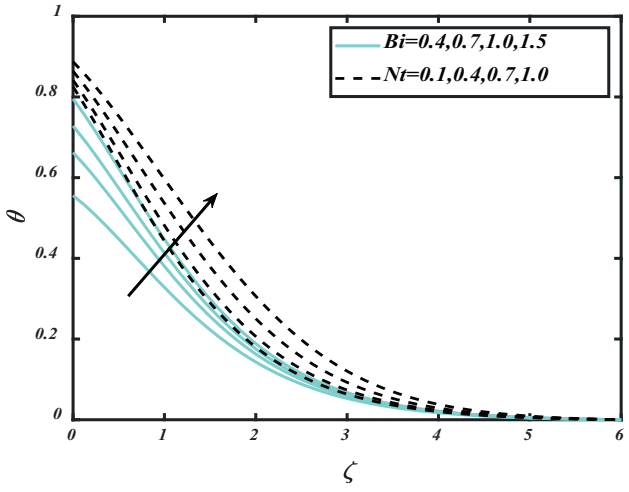

Fig. 5. θ against Bi & Nt.

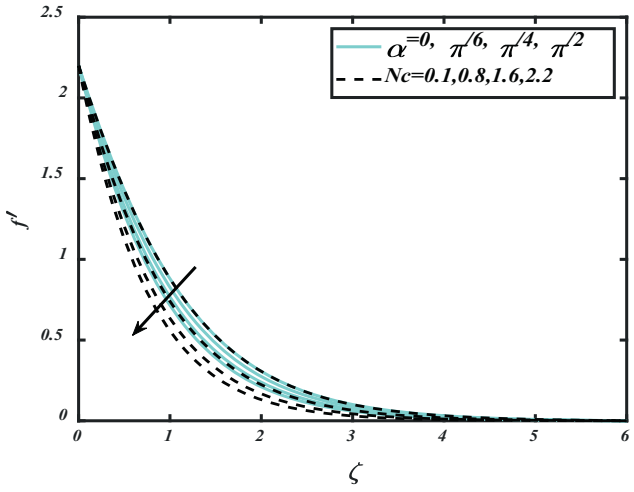

Fig. 3. f' againstα & Nc.

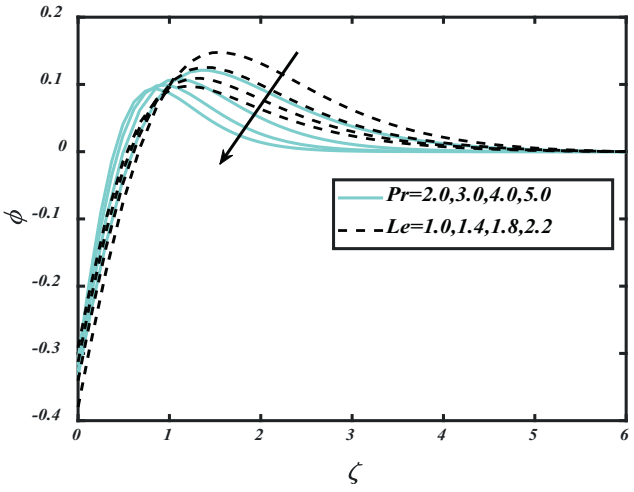

Fig. 6. ϕ against Pr & Le.

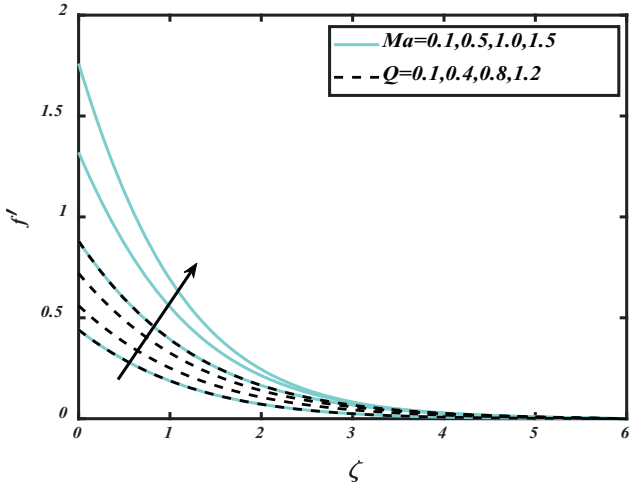

Fig. 4. f' against Ma & Q.

nanofluid, bioconvection transpiration and thermal radiation. In Figs. 1-10, the effects of physical factors like magnetic parameter (M), energy parameter for activation (E), bouncy ratio parameter (Nr), thermophoresis parameter (Nt), Prandtl number (Pr), chemical reaction parameter (σ), microorganism variation parameter (δ_1), Peclet number (Pe), mixed parameter convection (λ), Lewis bio convenient number (Lb), Rayleigh bioconvection number (Nc), Brownian motion parameter (Nb), wedge parameter (n), Lewis number (Le), second grade fluid parameter (β), wedge angle (α), Marangoni number (Q), and Marangoni ratio parameter (Ma) is presented. Fig. 1 displays the characteristics of the Nrbounce ratio parameter and second-degree velocity f' fluid parameter β. We may notice that the velocityf'field is enhanced by a bigger second-degree fluidβ, while the bouncy ratio parameterNr is reduced. Fig. 2 illustrates the impact of the wedge n and the velocity field parameterλ. The rising mixed convection parameter λ is apparent in Fig. 3 and wedge parameter n raises the velocity field f'. Fig. 3 shows the result of the Rayleigh Number Nc and Wedge Corner Parameter α on the velocity profile f'. The wedge angle parameter α may be examined and Nc the fluid movement reduces. The influence of the Marangoni ratio Ma and Marangoni numbers Q on velocity distribution f' is seen in Fig. 4. With the Marangoni ratio parameter Ma, the velocity field f' increases with the predicted intensification. The velocity profile f is analyzed from these curves while the number of Marangoni Q is improved. Fig. 5

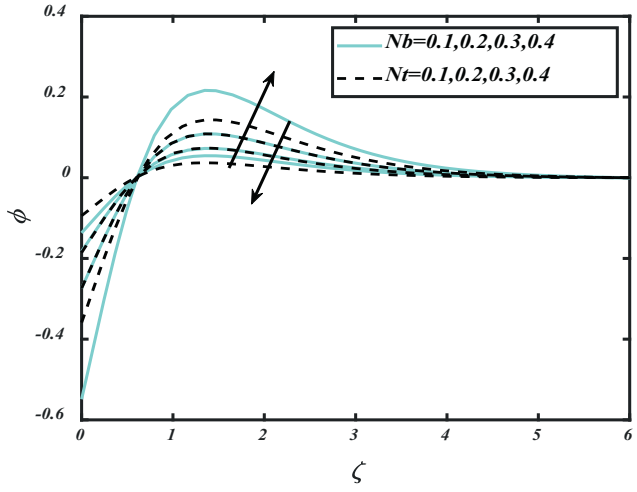

Fig. 7. ϕ against *Nb* & *Nt*.

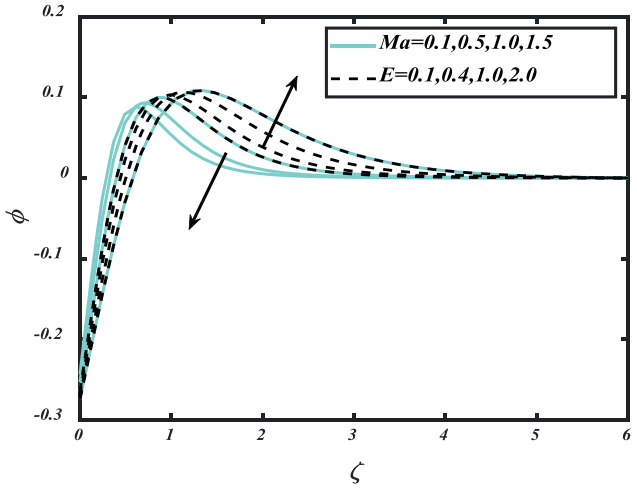

Fig. 8. ϕ against *Ma* & *E*.

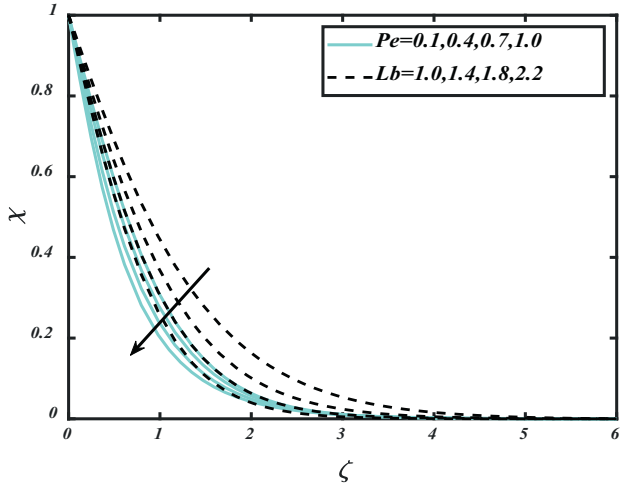

Fig. 9. χ against *Pe* & *Lb*.

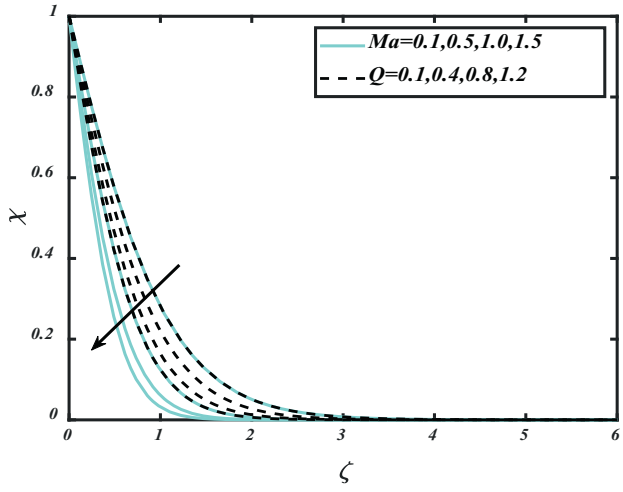

Fig. 10. χ against*Ma* & *Q*.

Table 1
Numerical solutions of $-f'(0)$ versus physical parameters.

M	λ	*Nr*	*Nc*	*Q*	*Ma*	β_1	$-f'(0)$
0.1	0.2	0.5	0.5	1.0	0.1	0.1	1.7962
0.2							1.8499
0.3							1.9018
0.5	0.4	0.5	0.5	1.0	0.1	0.1	2.0466
	0.8						
	1.2						2.0773
							2.1081
0.5	0.2	0.1	0.5	1.0	0.1	0.1	2.0333
		0.2					
		0.3					2.0327
							2.0322
0.5	0.2	0.5	0.1	1.0	0.1	0.1	2.0656
			0.2				
			0.3				2.0435
							2.0243
0.5	0.2	0.5	0.5	2.0	0.1	0.1	2.9866
				3.0			3.5344
				4.0			4.5317
0.5	0.2	0.5	0.5	1.0	0.2	0.1	2.2697
					0.5		3.0233
					0.8		3.8323
0.5	0.2	0.5	0.5	1.0	0.1	0.2	3.7269
						0.4	3.5243
						0.8	3.1553

depicts the temperature distribution θ with Biot number *Bi* and thermophoresis parameter *Nt*. Temperature distribution expands as the magnitudes of the Biot number *Bi* and thermophoresis parameter *Nt* rise. Fig. 6 shows the profile and Pr Lewis number fluctuation concentrationϕ. The concentration ϕ is declining with the increased estimate Prand number of Lewis *Le*. Fluctuating nanoparticles ϕ volumetry through Brownian motion parameter *Nb* and thermophoresis parameter is shown in Fig. 7. It is discovered that with Brown's motion parameter the solute field of nanoparticles ϕ decreases. This figure shows the concentration field ϕ increased by increasing the thermophoresis parameter *Nt* values. From this figure. Physically, the random motion of the particles increases by improving Brownian motion parameter because of a collision of the particles. As a result, the profile of concentration decreases. The impact on volumetric concentration of nanoparticles ϕ of the parameter of Marangoni ratio *Ma* and activation energy*E* is investigated in Fig. 8. The Marangoni ratio parameter *Ma* is analyzed for nanoparticles ϕ concentration increases with a bigger, but declining nature. Fig. 9 indicates a reduction in the fields of microorganisms χ becoming bigger *Pe* and *Lb* larger. Fig. 10 shows the field of

Table 2
Numerical solutions of $-\theta'(0)$ versus physical parameters.

M	Nt	Pr	Q	Ma	β_1	Rd	$-\theta'(0)$
0.1	0.3	2.0	1.0	0.1	0.1	0.4	0.5280
0.2							0.5275
0.3							0.5270
0.5	0.1	2.0	1.0	0.1	0.1	0.4	0.5467
	0.4						0.5152
	0.9						0.4586
0.5	0.3	2.6	1.0	0.1	0.1	0.4	0.6171
		3.2					0.6869
		3.8					0.7429
0.5	0.3	2.0	2.0	0.1	0.1	0.4	0.6608
			3.0				0.7386
			4.0				0.7922
0.5	0.3	2.0	1.0	0.2	0.1	0.4	0.5425
				0.5			0.5861
				0.8			0.6217
0.5	0.3	2.0	1.0	0.1	0.2	0.4	0.6225
					0.4		0.6239
					0.8		0.6265
0.5	0.3	2.0	1.0	0.1	0.1	0.5	0.5151
						0.8	0.4858
						1.0	0.4686

Table 3
Numerical solutions of $\phi'(0)$ versus physical parameters.

M	Nt	Pr	Q	Ma	β_1	Le	Nb	$\phi'(0)$
0.1	0.3	2.0	1.0	0.1	0.1	2.0	0.2	0.7920
0.2								0.7912
0.3								0.7904
0.5	0.1	2.0	1.0	0.1	0.1	2.0	0.2	0.2733
	0.4							1.0304
	0.9							2.0638
0.5	0.3	2.6	1.0	0.1	0.1	2.0	0.2	0.9256
		3.2						1.0303
		3.8						1.1143
0.5	0.3	2.0	2.0	0.1	0.1	2.0	0.2	0.9912
			3.0					1.1079
			4.0					1.1883
0.5	0.3	2.0	1.0	0.2	0.1	2.0	0.2	0.8137
				0.5				0.8791
				0.8				0.9326
0.5	0.3	2.0	1.0	0.1	0.2	2.0	0.2	0.9337
					0.4			0.9359
					0.8			0.9397
0.5	0.3	2.0	1.0	0.1	0.1	2.2	0.2	0.7873
						2.4		0.7859
						2.6		0.7847
							0.1	1.5776
							0.4	0.3945
							0.9	0.1753

variation in the Marangoni Q and Marangoni ratio parameters Ma. With a growing estimation of the parameters Ma of the Marangoni ratio and the number of Marangoni Q, the field of microorganisms χ has declined.

Tables 1–4 are drawn out to examine the performance of several prominently determined flow parameters by local coefficient of skin friction, local number Nusselt and local numbers Sherwood. Table 1 clarifies local skin friction coefficient variations via various factors M, λ, Nr, Nc, Q, Ma and β_1. Greater values are investigated in order to M, λ, Q improve the local skin friction factor $-f''(0)$ while β_1 decreasing the local skin friction factor $-f''(0)$. Table 2 shows local numbers compared to Nusselt, and local Nusselt M, Nt, Pr , Rd, Q, Ma and β_1 populations have been checked to have decreased Rd, M, whereas Pr, Q, Ma and β_1 increases have occurred. The meta analysis regarding the flow of heated nanoparticles was presented in [21,22]. Table 3 summarizes the decline in M, Le and the growth of Nt, Pr the local Sherwood population. Table 4 shows that the number of microorganisms is increasing at an alarming rate Pe, Lb, Q and Ma.

Table 4
Numerical solutions of $-\chi'(0)$ versus physical parameters.

M	Q	Ma	β_1	Lb	Pe	$-\chi'(0)$
0.1	1.0	0.1	0.1	2.0	0.1	1.5472
0.2						1.5422
0.3						1.5374
0.5	2.0	0.1	0.1	2.0	0.1	2.1855
	3.0					2.6896
	4.0					3.1141
0.5	1.0	0.2	0.1	2.0	0.1	1.5964
		0.5				1.7934
		0.8				1.9709
0.5	1.0	0.1	0.2	2.0	0.1	1.9761
			0.4			1.9864
			0.8			2.0058
0.5	1.0	0.1	0.1	3.0	0.1	1.9044
				4.0		2.2217
				5.0		2.5012
					0.2	1.5911
					0.6	1.8475
					1.0	2.1102

5. Summary

In the occurrence of wedge-shaped geometry, the characteristics heat radiation and activation energy in the two-dimensional bioconvection flow of second-grade nanofluid including microorganisms. The following are the main points:

- The change in second-grade fluid parameter improved the velocity field while it reduce with the bouncy ratio parameters.
- When the number of Marangoni is improved, the velocity profile rises.
- As the magnitude of the Biot number rises, so does the temperature distribution.
- The concentration field increased when the thermophoresis parameter values increased.
- Compared to the greater bioconvection number Lewis and Peclet number, the microorganism field diminishes.
- The field of microorganisms is said to be reduced, with the Marangoni ratio parameter progressively estimated.

Author statement

All authors of the subjected paper is agreed to submit a manuscript in Journal of King Saud University-Science.

Declaration of Competing Interest

The authors declare that they have no known competing financial interests or personal relationships that could have appeared to influence the work reported in this paper.

References

[1] S.U.S. Choi, Enhancing thermal conductivity of fuids with nanoparticles, ASME Pub Fed. 231 (1995) 99–106.
[2] J. Boungiorno, L.W. Hu, S.J. Kim, R. Hannink, B. Truong, E. Forrest, Nanofluids for enhanced economics and safety of nuclear reactors: an evaluation of potential features, issues, and research gaps, Nucl. Technol. 162 (2008) 80–91.
[3] S. Lahmar, M. Kezzar, M.R. Eid, M.R. Sari, Heat transfer of squeezing unsteady nanofluid flow under the effects of an inclined magnetic field and variable thermal conductivity, Phys. A: Stat. Mech. Appl. 540 (2020) 123138.
[4] E.O. Fatunmbi, A.T. Adeosun, Nonlinear radiative Eyring-Powell nanofluid flow along a vertical Riga plate with exponential varying viscosity and chemical reaction, Int. Commun. Heat Mass Transfer 119 (2020) 104913.
[5] A. Shafiq, I. Khan, G. Rasool, E.S.M. Sherif, A.H. Sheikh, Influence of single-and multi-wall carbon nanotubes on magnetohydrodynamic stagnation point nanofluid flow over variable thicker surface with concave and convex effects, Mathematics 8 (1) (2020) 104.

[6] K. Loganathan, S. Rajan, An entropy approach of Williamson nanofluid flow with joule heating and zero nanoparticle mass flux, J. Therm. Anal. Calorim. (2020) 1–14.
[7] A. Hamid, Terrific effects of Ohmic-viscous dissipation on Casson nanofluid flow over a vertical thin needle: buoyancy assisting & opposing flow, J. Mater. Res. Technol. 9 (5) (2020) 11220–11230.
[8] S. Aman, I. Khan, Z. Ismail, M.Z. Salleh, Applications of fractional derivatives to nanofluids: exact and numerical solutions, Math. Model. Nat. Phenom. 13 (1) (2018) 2.
[9] M. Turkyilmazoglu, Single phase nanofluids in fluid mechanics and their hydrodynamic linear stability analysis, Comput. Methods Prog. Biomed. 187 (2020) 105171.
[10] R. Ellahi, F. Hussain, S.A. Abbas, M.M. Sarafraz, M. Goodarzi, M.S. Shadloo, Study of two-phase newtonian nanofluid flow hybrid with hafnium particles under the effects of slip, Inventions 5 (1) (2020) 6.
[11] Nadeem Abbas, S. Nadeem, Anber Saleem, M.Y. Malik, Alibek Issakhov, Fahd M. Alharbi, Models base study of inclined MHD of hybrid nanofluid flow over nonlinear stretching cylinder, Chin. J. Phys. 69 (February 2021) 109–117.
[12] S. Nadeem, Muhammad Israr-ur-Rehman, S. Saleem, Ebenezer Bonyah, Dual solutions in MHD stagnation point flow of nanofluid induced by porous stretching/shrinking sheet with anisotropic slip, AIP Adv. 10 (065207) (2020).
[13] Sabir Ali Shehzad, Sami Ullah Khan, Z. Abbas, A. Rauf, A revised Cattaneo-Christov micropolar viscoelastic nanofluid model with combined porosity and magnetic effects, Appl. Math. Mech. 41 (2020) 521–532.
[14] Muhammad Danish Ikram, Muhammad Imran Asjad, Ali Akgül, Dumitru Baleanu, Effects of hybrid nanofluid on novel fractional model of heat transfer flow between two parallel plates, Alex. Eng. J. 60 (4) (August 2021) 3593–3604.
[15] S. Qayyum, M. Ijaz Khan, T. Hayat, A. Alsaedi, M. Tamoor, Entropy generation in dissipative flow of Williamson fluid between two rotating disks, Int. J. Heat Mass Transf. 127 (2018) 933–942.
[16] Kh. Hosseinzadeh, So. Roghani, A.R. Mogharrebi, A. Asadi, M. Waqas, D.D. Ganji, Investigation of cross-fluid flow containing motile gyrotactic microorganisms and nanoparticles over a three-dimensional cylinder, Alex. Eng. J. 59 (5) (October 2020) 3297–3307.
[17] M. Ijaz Khan, Transportation of hybrid nanoparticles in forced convective Darcy-Forchheimer flow by a rotating disk, Int. Commun. Heat Mass Transfer 122 (March 2021) 105177.
[18] Ying-Qing Song, B.D. Obideyi, Nehad Ali Shah, I.L. Animasaun, Y.M. Mahrous, Jae Dong Chung, Significance of haphazard motion and thermal migration of alumina and copper nanoparticles across the dynamics of water and ethylene glycol on a convectively heated surface, Case Stud. Therm. Eng. 26 (August 2021) 101050.
[19] A.S. Oke, I.L. Animasaun, W.N. Mutuku, M. Kimathi, Nehad Ali Shah, S. Saleem, Significance of Coriolis force, volume fraction, and heat source/sink on the dynamics of water conveying 47 nm alumina nanoparticles over a uniform surface, Chin. J. Phys. 71 (June 2021) 716–727.
[20] Yun-Xiang Li, Hassan Waqas, Kamel Al-Khaled, Shan Ali Khan, M. Ijaz Khan, Sami Ullah Khan, Rabia Naseem, Yu-Ming Chu, Simultaneous features of Wu's slip, nonlinear thermal radiation and activation energy in unsteady bio-convective flow of Maxwell nanofluid configured by a stretching cylinder, Chin. J. Phys. 73 (October 2021) 462–478.
[21] I.L. Animasaun, R.O. Ibraheem, B. Mahanthesh, H.A. Babatunde, A meta-analysis on the effects of haphazard motion of tiny/nano-sized particles on the dynamics and other physical properties of some fluids, Chin. J. Phys. 60 (August 2019) 676–687.
[22] A. Wakif, I.L. Animasaun, P.V. Satya Narayana, G. Sarojamma, Meta-analysis on thermo-migration of tiny/nano-sized particles in the motion of various fluids, Chin. J. Phys. 68 (December 2020) 293–307.
[23] Nehad Ali Shah, I.L. Animasaun, Jae Dong Chung, Abderrahim Wakif, F.I. Alao, C.S.K. Raju, Significance of nanoparticle's radius, heat flux due to concentration gradient, and mass flux due to temperature gradient: The case of Water conveying copper nanoparticles, Sci. Rep. 11 (2021). Article number: 1882.
[24] G. Sowmya, B.J. Gireesha, I.L. Animasaun, Nehad Ali Shah, Significance of buoyancy and Lorentz forces on water-conveying iron(III) oxide and silver nanoparticles in a rectangular cavity mounted with two heated fins: heat transfer analysis, J. Therm. Anal. Calorim. 144 (2021) 2369–2384.
[25] O.D. Makinde, I.L. Animasaun, Bioconvection in MHD nanofluid flow with nonlinear thermal radiation and quartic autocatalysis chemical reaction past an upper surface of a paraboloid of revolution, Int. J. Therm. Sci. 109 (November 2016) 159–171.
[26] O.D. Makinde, I.L. Animasaun, Thermophoresis and Brownian motion effects on MHD bioconvection of nanofluid with nonlinear thermal radiation and quartic chemical reaction past an upper horizontal surface of a paraboloid of revolution, J. Mol. Liq. 221 (September 2016) 733–743.
[27] A.V. Kuznetsov, Nanofluid bioconvection in water-based suspensions containing nanoparticles and oxytactic microorganisms: oscillatory instability, Nanoscale Res. Lett. 6 (1) (2011 Dec 1) 100.
[28] M.K. Nayak, J. Prakash, D. Tripathi, V.S. Pandey, S. Shaw, O.D. Makinde, 3D Bioconvective multiple slip flow of chemically reactive Casson nanofluid with gyrotactic micro-organisms, Heat Transf.—Asian Res. 49 (1) (2020 Jan) 135–153.
[29] S.U. Khan, H. Waqas, M.M. Bhatti, M. Imran, Bioconvection in the rheology of magnetized couple stress Nanofluid featuring activation energy and Wu's slip, J. Non-Equilibrium Thermodyn. 45 (1) (2020 Jan 28) 81–95.
[30] V.M. Magagula, S. Shaw, R.R. Kairi, Double dispersed bioconvective Casson nanofluid fluid flow over a nonlinear convective stretching sheet in suspension of gyrotactic microorganism, Heat Transfer 49 (5) (2020) 2449–2471.
[31] O.A. Beg, M. Aneja, S.A.P.N.A. Sharma, S. Kuharat, Computation of electro-conductive gyrotactic bioconvection from a nonlinear inclined stretching sheet under non-uniform magnetic field: simulation of smart bio-nano-polymer coatings for solar energy, Int. J. Mod. Phys. B 34 (05) (2020), 2050028.
[32] S.U. Mamatha, K. Ramesh Babu, P. Durga Prasad, C.S.K. Raju, S.V.K. Varma, Mass transfer analysis of two-phase flow in a suspension of microorganisms, Arch. Thermodyn. (2020) 175–192.
[33] N.I. Nima, S.O. Salawu, M. Ferdows, M.D. Shamshuddin, A. Alsenafi, A. Nakayama, Melting effect on non-Newtonian fluid flow in gyrotactic microorganism saturated non-darcy porous media with variable fluid properties, Appl. Nanosci. 10 (10) (2020) 3911–3924.
[34] M. Ramzan, H. Gul, J.D. Chung, S. Kadry, Y.M. Chu, Significance of Hall effect and Ion slip in a three-dimensional bioconvective Tangent hyperbolic nanofluid flow subject to arrhenius activation energy, Sci. Rep. 10 (1) (2020) 1–15.
[35] I. Tlili, H. Waqas, A. Almaneea, S.U. Khan, M. Imran, Activation energy and second order slip in bioconvection of Oldroyd-B nanofluid over a stretching cylinder: a proposed mathematical model, Processes. 7 (12) (2019 Dec) 914.
[36] T. Hayat, S.A. Khan, M.I. Khan, A. Alsaedi, Optimizing the theoretical analysis of entropy generation in flow of second grade nanofluid, Phys. Scr. 94 (2019), 085001.
[37] M.I. Khan, F. Alzahrani, A. Hobiny, Z. Ali, Fully developed second order velocity slip Darcy-Forchheimer flow by a variable thicked surface of disk with entropy generation, Int. Commun. Heat Mass Transfer 117 (2020) 104778.
[38] T. Hayat, N. Aslam, M.I. Khan, M.I. Khan, A. Alsaedi, Physical significance of heat generation/absorption and Soret effects on peristalsis flow of pseudoplastic fluid in an inclined channel, J. Mol. Liq. 275 (2019) 599–615.
[39] M.I. Khan, F. Alzahrani, A. Hobiny, A. Ali, Modeling of Cattaneo-Christov double diffusions (CCDD) in Williamson nanomaterial slip flow subject to porous medium, J. Mater. Res. Technol. 9 (2020) 6172–6177.
[40] M.I. Khan, F. Alzahrani, Nonlinear dissipative slip flow of Jeffrey nanomaterial towards a curved surface with entropy generation and activation energy, Math. Comput. Simul. 185 (2021) 47–61.